4804 *Biochemistry* **2010,** *49,* 4804–4812
DOI: 10.1021/bi100207k

BIOCHEMISTRY
including biophysical chemistry & molecular biology
Article

μ-Conotoxin KIIIA Derivatives with Divergent Affinities versus Efficacies in Blocking Voltage-Gated Sodium Channels[†]

Min-Min Zhang,[‡] Tiffany S. Han,[‡] Baldomero M. Olivera,[‡] Grzegorz Bulaj,[§] and Doju Yoshikami*[,‡]

[‡]*Department of Biology, University of Utah, Salt Lake City, Utah 84112, and* [§]*Department of Medicinal Chemistry, University of Utah, Salt Lake City, Utah 84108*

Received February 10, 2010; Revised Manuscript Received April 19, 2010

ABSTRACT: The possibility of independently manipulating the affinity and efficacy of pore-blocking ligands of sodium channels is of interest for the development of new drugs for the treatment of pain. The analgesic μ-conotoxin KIIIA (KIIIA), a 16-residue peptide with three disulfide bridges, is a pore blocker of voltage-gated sodium channels, including neuronal subtype $Na_V1.2$ (K_d = 5 nM). At saturating concentrations, KIIIA incompletely blocks the sodium current of $Na_V1.2$, leaving a 5% residual current ($r I_{Na}$). Lys7 is an important residue: the K7A mutation decreases both the efficacy (i.e., increases $r I_{Na}$ to 23%) and the affinity of the peptide (K_d = 115 nM). In this report, various replacements of residue 7 were examined to determine whether affinity and efficacy were inexorably linked. Because of their facile chemical synthesis, KIIIA analogues that had as a core structure the disulfide-depleted KIIIA[C1A,C2U,C9A,C15U] (where U is selenocysteine) or ddKIIIA were used. Analogues ddKIIIA and ddKIIIA[K7X], where X represents one of nine different amino acids, were tested on voltage-clamped *Xenopus* oocytes expressing rat $Na_V1.2$ or $Na_V1.4$. Their affinities ranged from 0.01 to 36 μM and $r I_{Na}$ values from 2 to 42%, and these two variables appeared to be uncorrelated. Instead, $r I_{Na}$ varied inversely with side chain size, and remarkably charge and hydrophobicity appeared to be inconsequential. The ability to manipulate a μ-conopeptide's affinity and efficacy, as well as its capacity to interfere with subsequent tetrodotoxin binding, greatly expands its scope as a reagent for probing sodium channel structure and function and may also lead to the development of μ-conotoxins as safe analgesics.

Voltage-gated sodium channels (VGSCs)[1] are responsible for the upstroke of action potentials, which mediate rapid communication of electrical signals in neuron and muscle (*1*). Mammals have nine isoforms of the pore-forming α-subunit of VGSCs ($Na_V1.1-Na_V1.9$) and four isoforms of associated β-subunits ($\beta1-\beta4$) (*2*−*4*). The importance of VGSCs is reflected by the fact that they are targets of many neurotoxins that have convergently evolved in a variety of organisms (*5*−*8*). These neurotoxins are of considerable interest not only as probes for investigating the functioning of these channels but also as potential therapeutics for neurological disorders, including neuropathic pain and epilepsy (*9*, *10*).

Four families of VGSC-targeting conopeptides, each with a distinct mechanism of action, are known: μ-, μO-, δ-, and ι-conotoxins. The first two are antagonists, and the latter two are agonists (*8*, *11*). These conopeptides have multiple disulfide bridges, with members of each family having a characteristic disulfide framework. Of these families, μ-conotoxins were the first to be discovered, and like the guanidinium alkaloids, tetrodotoxin (TTX) and saxitoxin (STX), are pore blockers that act at neurotoxin receptor site 1 (*8*, *12*−*15*). Among the more recently discovered members of this family is μ-conotoxin KIIIA (*16*). KIIIA has several distinctive features when compared with μ-conotoxin GIIIA, the first- and best-studied member of the family. (1) GIIIA has 22 residues, whereas KIIIA has 16 and is the smallest μ-conopeptide described so far (see Figure 1). (2) Unlike GIIIA, which has highest affinity for $Na_V1.4$ (the skeletal muscle-specific VGSC), KIIIA has the highest affinity for $Na_V1.2$ (a neuronal VGSC) (*17*). Furthermore, KIIIA also exhibits analgesic activity (*17*). (3) When GIIIA binds to $Na_V1.4$, it blocks the sodium current (I_{Na}) essentially completely; in contrast, when KIIIA binds $Na_V1.2$, a small residual sodium current ($^r I_{Na,}$ 5% of control) persists (*18*). (4) When the R13Q mutant of GIIIA, GIIIA[R13Q], binds to $Na_V1.4$, a finite $r I_{Na}$ of 28% is observed in single-channel recordings in planar lipid bilayers (*19*). A loss-of-positive-charge mutation at the presumed homologous location in KIIIA, K7A (see Figure 1), likewise increases $r I_{Na}$ (*18*). However, unlike the $r I_{Na}$ of GIIIA[R13Q], which could not be blocked by decarbamoyl-STX (*19*), the $r I_{Na}$ of both KIIIA and KIIIA[K7A] can be blocked by TTX (*18*) and decarbamoyl-STX (M.-M. Zhang et al., manuscript in preparation); thus, guanidinium alkaloid, KIIIA (or KIIIA[K7A]), and $Na_V1.2$ can form a ternary complex.

[†]This work was supported by National Institutes of Health Grants PO1 GM48677 (G.B., B.M.O., and D.Y.) and R21 NS055845 (G.B. and D.Y.).

*To whom correspondence should be addressed: Department of Biology, University of Utah, 257 S. 1400 E., Salt Lake City, UT 84112. E-mail: yoshikami@bioscience.utah.edu. Phone: (801) 581-3084. Fax: (801) 581-4668.

[1]Abbreviations: dap, diaminoproprionate; ddKIIIA, disulfide-depleted μ-conotoxin KIIIA, i.e., KIIIA[C1A,C2U,C9A,C5U], where U is selenocysteine; ddKIIIA[K7X], ddKIIIA with residue X in position 7; ddKIIIA·Na_V, binary complex of ddKIIIA and Na_V; ddKIIIA-[K7X]·Na_V, binary complex of ddKIIIA[K7X] and Na_V; ddKIIIA-[K7X]·TTX·Na_V, ternary complex of ddKIIIA[K7X], TTX, and Na_V; GIIIA, μ-conotoxin GIIIA; I_{Na}, sodium current; KIIIA, μ-conotoxin KIIIA; KIIIA[K7A], μ-conotoxin KIIIA[K7A]; Na_V, α-subunit of the voltage-gated sodium channel; $r I_{Na}$, residual sodium current; TTX, tetrodotoxin; TTX·Na_V, binary complex of TTX and Na_V; VGSC, voltage-gated sodium channel.

 Published on Web 05/11/2010

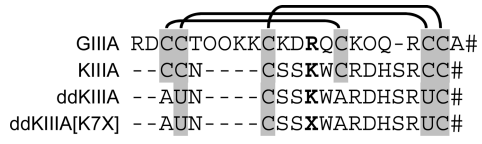

FIGURE 1: Aligned sequences of μ-conotoxins GIIIA, KIIIA, ddKIIIA, and ddKIIIA[K7X]. GIIIA and KIIIA have the three canonical disulfide bridges of μ-conotoxins: between the first and fourth, second and fifth, and third and sixth cysteine residues (as indicated by lines above the sequences). ddKIIIA and ddKIIIA[K7X] have the same bridge framework except the first disulfide bridge was deleted and the second was replaced with a diselenide bridge. The long moniker of ddKIIIA[K7X] is KIIIA[C1A,C2U,K7X,C9A,C15U], where residue X at position 7 was either Ala, Asp, Gly, Leu, Lys (i.e., ddKIIIA), Phe, Ser, Thr, Val, or diaminoproprionate (dap). Abbreviations: O, hydroxyproline; #, amide; U, selenocysteine; shading, disulfide- or diselenide-bridged residues.

The K7A mutation in KIIIA not only increased rI_{Na} but also increased the peptide's K_d for $Na_V1.2$ (*18*); thus, the mutation decreased both efficacy and affinity, raising the possibility that affinity and efficacy might be immutably linked. In this report, we investigated this further by positional scanning. Exploration of the structure−activity relationships of multiply disulfide-bonded peptides, such as μ-conotoxins, requires correctly folding each synthetic peptide, a time-consuming and laborious process. Therefore, we employed a newly developed method for the facile synthesis of disulfide-bonded peptides that exploits two recent observations. (1) The first disulfide bridge, that formed by the first and fourth cysteines of KIIIA, can be removed with only modest attenuation of functional activity (*20*), and (2) a diselenide bridge can be substituted for one of the disulfide bridges, which results in a construct that is significantly easier to fold (*21*). With regard to the latter, it is noteworthy that the selenopeptide derivatives of α-, ω-, and μ-conopeptides have recently been shown to retain bioactivities of their native conotoxin counterparts (*22*−*24*). Incorporation of both modifications into KIIIA results in the disulfide-depleted peptide KIIIA[C1A,C2U,C9A, C15U] [where U represents selenocysteine (see Figure 1)] or ddKIIIA, which retains functional activity (*25*). Thus, ddKIIIA served as a more readily synthesized surrogate of KIIIA and was used as a core structure for positional scanning; specifically, the residue at position 7 was mutated to form ddKIIIA[K7X], where X was one of nine amino acids differing in size, charge, or hydrophobicity. This investigation showcases the usefulness of disulfide-depleted, selenocysteine-substituted peptides and at the same time reveals that derivatives of KIIIA with divergent affinities versus efficacies could be synthesized. These properties are particularly interesting, since the KIIIA is an analgesic (*17*) with possibilities as a lead compound in the development of potential therapeutics for the treatment of pain.

MATERIALS AND METHODS

Oocyte Electrophysiology. Oocytes expressing $Na_V1.2$ or $Na_V1.4$ were prepared and voltage-clamped essentially as previously described (*11*, *17*). Briefly, a given oocyte was injected with 30 nL of cRNA of rat $Na_V1.2$ or rat $Na_V1.4$ (1.5 or 0.6 ng, respectively) and incubated for 1−4 days at 16 °C in ND96 composed of 96 mM NaCl, 2 mM KCl, 1.8 mM $CaCl_2$, 1 mM $MgCl_2$, and 5 mM HEPES (pH 7.5). The incubation medium also contained the antibiotics penicillin (100 units/mL), streptomycin (0.1 mg/mL), amikacin (0.1 mg/mL), and Septra (0.2 mg/mL). Oocytes in ND96 were two-electrode voltage-clamped using microelectrodes containing 3 M KCl (< 0.5 MΩ) and held a membrane potential of −80 mV. Sodium channels were activated when the potential was stepped to −10 mV (unless otherwise specified) for 50 ms every 20 s. Current signals were filtered at 2 kHz, digitized at a sampling frequency of 10 kHz, and leak-subtracted by a P/8 protocol using in-house software written in LabVIEW (National Instruments, Austin, TX).

The oocyte recording chamber consisted of a well (4 mm diameter, 30 μL volume) in Sylgard (Dow Corning, Midland, MI), a silicone elastomer. Oocytes were exposed to toxin via application of 3 μL of toxin at 10 times its final concentration with a pipettor, and the bath was manually stirred for a few seconds by gentle aspiration and expulsion of a few microliters of the bath fluid several times with the pipettor. Toxin exposures were in a static bath to conserve material. The toxin-containing solution was washed out of the well by perfusion with ND96, initially at a speed of 1.5 mL/min for ∼20 s, and then at 0.5 mL/min thereafter. Recordings were conducted at room temperature.

Toxins. All peptides were synthesized on a solid support using the *N*-(9-fluorenyl)methoxycarbonyl (Fmoc) chemistry as described previously (*20*). In particular, ddKIIIA and its derivatives were synthesized as recently described (*25*). Briefly, selenocysteine residues were protected with *p*-methoxybenzyl groups (Chem-Impex International, Wood Dale, IL). Analogues were removed from the resin via a 3 h treatment with a modified reagent K consisting of trifluoroacetic acid (TFA), thioanisole, phenol, and water (90:2.5:7.5:2.5, v/v/v/v) and 1.3 equiv of DTNP [2,2′-dithiobis(5-nitropyridine)]. The selenoconopeptide analogues were treated for 1 h with DTT (dithiothreitol, 100 mM), Tris [tris(hydroxymethyl)aminomethane, 0.1 M], and EDTA (ethylenediaminetetraacetic acid, 1 mM) (pH 7.5) at room temperature. The peptides were purified by reversed-phase high-performance liquid chromatography (HPLC). Oxidative folding was performed with a mixture of oxidized and reduced glutathione (1 mM GSSG and 1 mM GSH) in Tris-HCl (0.1 M, pH 7.5) and EDTA (1 mM) at room temperature. The oxidized peptide analogues were purified by C_{18} semipreparative HPLC. The chemical identity of each analogue was confirmed by mass spectrometry. TTX was purchased from Alomone Laboratories (Jerusalem, Israel). Lyophilized peptides were dissolved in ND96; lyophilized TTX was dissolved in water, and both were stored frozen until they were used.

Data Analysis. Unless otherwise specified, values of k_{on} were obtained from slopes of k_{obs} versus peptide concentration plots, and k_{off} values were obtained from single-exponential fits of recovery from block following peptide washout, as previously described (*26*). Unless otherwise indicated, averaged data in graphs and tables are means ± the standard deviation ($N \geq 3$ oocytes).

RESULTS

Affinities and Efficacies of ddKIIIA and Nine ddKIIIA-[K7X] Analogues in Blocking $Na_V1.2$. Synthetic peptides were synthesized and tested for their ability to inhibit voltage-gated sodium currents (I_{Na}) of voltage-clamped *Xenopus* oocytes expressing $Na_V1.2$ as described in Materials and Methods. When the peptides were tested at various concentrations, the resulting dose−response curves were fit well by the Langmuir adsorption isotherm (Figure 2), consistent with a bimolecular reaction between the peptide and channel; furthermore, the steady-state IC_{50} values were similar to the kinetically derived K_d values (Table 1).

At saturating concentrations, the maximum block produced by all of the peptides plateaued at a level below 100%; i.e., a residual current (rI_{Na}) persisted when the peptide was bound to the channel. In this regard, the peptides could be placed into two categories, those that blocked >90% (rI_{Na} < 10%) and those that were unable to block more than 86% ($rI_{Na} \geq 14\%$) (Table 1). For the sake of clarity, the dose−response curves of the peptides in each category are plotted separately in Figure 2.

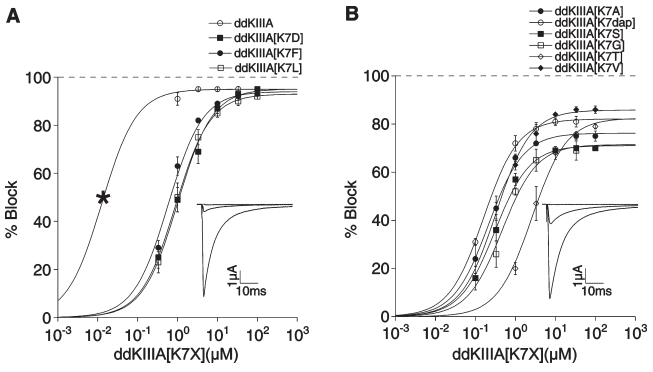

FIGURE 2: Saturating concentrations of ddKIIIA or ddKIIIA[K7X] block $Na_V1.2$ incompletely. Oocytes were voltage-clamped as described in Materials and Methods and exposed to peptide until steady-state block of sodium currents was achieved. Superimposed plots of analogues with (A) small (5−7%) rI_{Na} values, where X is K, D, F, or L, and (B) large (14−30%) rI_{Na} values, where X is A, S, G, T, V, or dap (diaminoproprionate). The asterisk in panel A (left-most data point for ddKIIIA) represents K_d, calculated from k_{off}/k_{on} (Table 1), since slow rates of block by ddKIIIA in that range of concentrations precluded accurate measurement of steady-state levels of block. Data points represent means ± the standard deviation ($N \geq 4$). Solid curves represent fits of data (including asterisk) to the equation for the Langmuir adsorption isotherm [$Y = 100 \times \text{plateau}/(1 + IC_{50}/[\text{peptide}])$]. IC_{50} and plateau (i.e., rI_{Na}) values are listed in Table 1. The insets show representative traces in response to a depolarizing step to −10 mV from a holding potential of −80 mV before treatment (control, large trace), in the presence of (attenuated trace) either 10 μM ddKIIIA (A) or 30 μM ddKIIIA[K7A] (B), and in the presence of both peptide and TTX (flat trace), where the residual current that persisted in the presence of peptide was obliterated by TTX (100 and 10 μM in panels A and B, respectively) (see also Figure 4C,D). Data in panels A and B are plotted separately for the sake of visual clarity.

The residual current resembled the control current in all respects except amplitude. Specifically, the time course as well as the $I-V$ curve of the rI_{Na} with ddKIIIA or ddKIIIA[K7A] were essentially the same as those of sodium currents under control conditions (Figure 3). These results show that the kinetics and voltage sensitivities of rI_{Na} are essentially indistinguishable from those of the control I_{Na} and are consistent with the peptides acting purely as pore blockers.

TTX Blocks the rI_{Na} with All Peptides Examined. The residual current, which persisted in saturating concentrations of all peptides tested, could be blocked by TTX, albeit more slowly than the rate at which TTX blocked control currents (Figure 4 and Table 2).

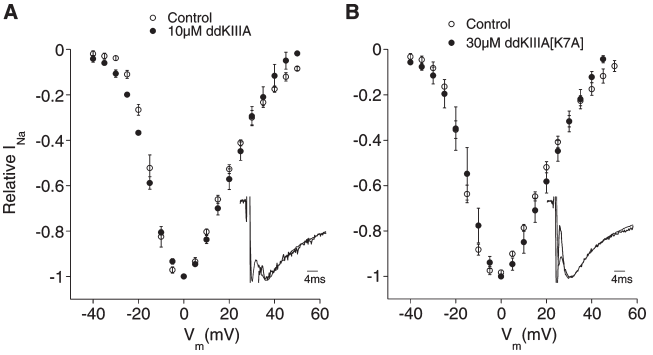

FIGURE 3: Kinetics and voltage dependence of rI_{Na} of $Na_V1.2$ with ddKIIIA or ddKIIIA[K7A] are essentially the same as those of control I_{Na}. Oocytes expressing $Na_V1.2$ were voltage-clamped and exposed to toxin essentially as described in the legend of Figure 2. $I-V$ curves of control I_{Na} (○) and rI_{Na} (●) with ddKIIIA (A) and ddKIIIA[K7A] (B) have essentially the same profile and indicate that the gating properties of the channel were minimally, if at all, affected by the presence of the peptides. To ensure that control I_{Na} and rI_{Na} values were obtained with comparable voltage-clamp fidelity, control currents were obtained from oocytes that provided small I_{Na} values with amplitudes comparable to those of rI_{Na} (~200 and ~500 nA for ddKIIIA and ddKIIIA[K7A], respectively). Insets show normalized averaged traces of control I_{Na} (gray) and rI_{Na} (black) with ddKIIIA (A) and ddKIIIA[K7A] (B) illustrating that rI_{Na} and control I_{Na} have essentially the same time course (the first few milliseconds of the traces represent capacitative transients to be ignored). Data are means ± the standard deviation from at least three oocytes.

Table 1: Kinetics, Affinities, and Efficacies of ddKIIIA and Analogues in Blocking $Na_V1.2$[a]

peptide	k_{on} (μM^{-1} min^{-1})	k_{off} (min^{-1})	K_d (μM)	IC_{50} (μM) (95% confidence interval)	rI_{Na}[d] (%)
ddKIIIA	0.75 ± 0.015	0.01 ± 0.0015	0.013 ± 0.002	NA[c]	5 ± 1.1
ddKIIIA[K7A]	0.69 ± 0.11	0.13 ± 0.03	0.19 ± 0.05	0.21 (0.17−0.25)	24 ± 2.1
ddKIIIA[K7D]	0.08 ± 0.005	0.083 ± 0.02	1.04 ± 0.26	1 (0.85−1.2)	5 ± 2.4
ddKIIIA[K7S]	0.77 ± 0.07	0.11 ± 0.02	0.14 ± 0.03	0.31 (0.26−0.37)	29 ± 1.7
ddKIIIA[K7F]	0.55 ± 0.05	0.3 ± 0.04	0.55 ± 0.09	0.6 (0.52−0.7)	6 ± 2.0
ddKIIIA[K7G]	1.2 ± 0.1	0.67 ± 0.11	0.56 ± 0.1	0.47 (0.36−0.6)	29 ± 2.6
ddKIIIA[K7L]	0.39 ± 0.15	0.2 ± 0.009	0.51 ± 0.2	0.87 (0.76−1.0)	7 ± 1.7
ddKIIIA[K7V]	0.33 ± 0.018	0.091 ± 0.014	0.28 ± 0.045	0.34 (0.3−0.38)	14 ± 1.4
ddKIIIA[K7T]	0.1 ± 0.015	0.09 ± 0.006	0.9 ± 0.15	2.3 (1.8−3.0)	19 ± 3.3
ddKIIIA[K7dap]	1.2 ± 0.06	0.06 ± 0.008	0.05 ± 0.007	0.13 (0.09−0.19)	18 ± 1.3
KIIIA[b]	0.3 ± 0.03	0.0016 ± 0.0016	0.0053 ± 0.005	NA[c]	5 ± 3
KIIIA[K7A][b]	0.13 ± 0.006	0.015 ± 0.005	0.115 ± 0.038	NA[c]	23 ± 1
KIIIA[K7D]	0.02 ± 0.002	0.008 ± 0.001	0.4 ± 0.06	NA[c]	6 ± 2.0

[a]Rate constants were determined as described in Materials and Methods. Steady-state IC_{50} and rI_{Na} values were obtained with the data and equation presented in Figure 2. The standard deviations and 95% confidence intervals were calculated from at least three independent experiments using Prism. For comparison, also shown are data for KIIIA and KIIIA[K7A] from ref *18*. [b]Data from ref *18*. [c]The IC_{50} value was not obtained, because the rates of block using peptide concentrations in the range of the expected IC_{50} were too slow to provide accurate steady-state levels of block within the time frame of the experiments. [d]rI_{Na} values for ddKIIIA, KIIIA, and KIIIA[K7A] were directly measured using a saturating peptide concentration, and those for the remaining peptides represent the plateaus of the best-fit curves as described in the legend of Figure 2.

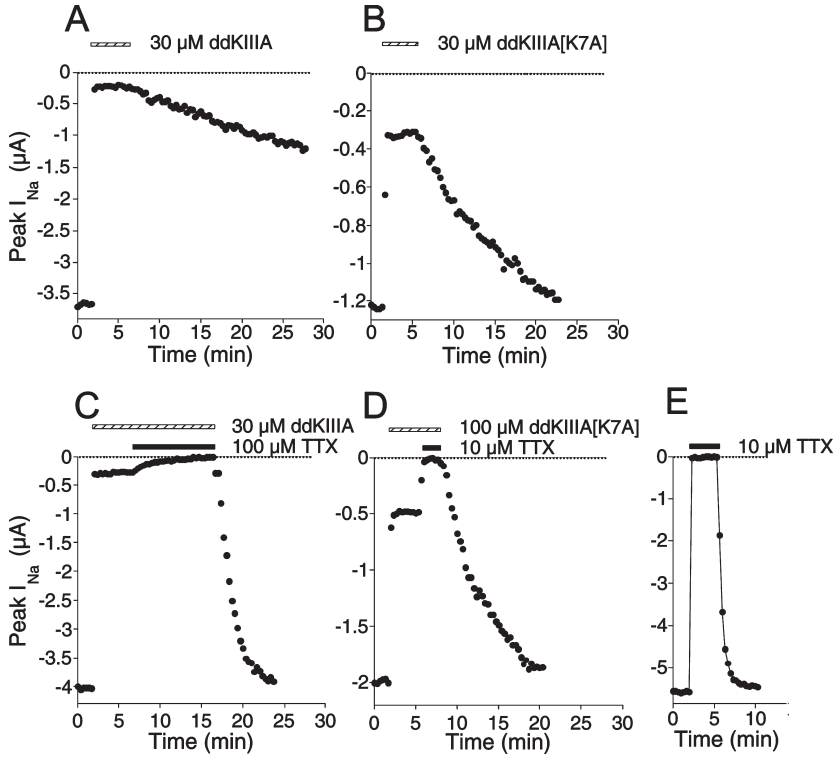

FIGURE 4: Kinetics of block of I_{Na} of $Na_V1.2$ by ddKIIIA or ddKIIIA[K7A] and kinetics of block of respective rI_{Na} by TTX. Oocytes expressing $Na_V1.2$ were voltage-clamped, and current recordings were obtained every 20 s as described in Materials and Methods. Example plot of peak sodium currents (I_{Na}) vs time during exposure to and washout of a saturating concentration (30 μM) of ddKIIIA (A) or ddKIIIA[K7A] (B). Block by ddKIIIA and ddKIIIA[K7A] leveled off at $< 100\%$ (leaving rI_{Na} values of $\sim$5 and 25%, respectively), and washout of ddKIIIA[K7A] was faster than that of ddKIIIA. The preceding was repeated, except that after steady-state block had been obtained by each peptide, the bath was supplemented with TTX, either 100 or 10 μM with ddKIIIA (C) and ddKIIIA[K7A] (D). In each case, the rI_{Na} was completely blocked by TTX, albeit more slowly than upon exposure to 10 μM TTX alone (E). Following washout of both peptide and TTX, I_{Na} fully recovered with a time course faster than that following washout of the peptide alone (compare panel A with panel C and panel B with panel D) but more slowly than that following TTX alone (compare panels C and D with panel E). For all panels, the presence of TTX is indicated by black bar and that of peptide by a white bar. A different oocyte was used to acquire the data for each panel. Rate constants of block of rI_{Na} by TTX (k_{obs}) and recovery (k_{off}) for ddKIIIA and all ddKIIIA[K7X] derivatives are summarized in Table 2.

Comparison of k_{off} for recovery from block following toxin washout of the peptide·Na_V binary complex with that of the peptide·TTX·Na_V ternary complex indicates that the presence of TTX accelerated the recovery from block when the peptide was ddKIIIA (58-fold increase in k_{off}), ddKIIIA[K7dap] (9-fold increase in k_{off}), or ddKIIIA[K7A] (2-fold increase in k_{off}). However, the presence of TTX did not significantly affect the k_{off} values for the remaining dd peptides (Table 2).

Affinities and Efficacies of KIIIA and Its Analogues in Blocking $Na_V1.4$. To examine the block by KIIIA and its analogues of a sodium channel isoform other than $Na_V1.2$, the effects of KIIIA, KIIIA[K7A], ddKIIIA, and all nine ddKIIIA-[K7X] peptides were also tested on $Na_V1.4$. The behavior of these peptides on $Na_V1.4$ qualitatively resembled that on $Na_V1.2$. Thus, the peptides could be placed in either of two categories with respect to rI_{Na} size (Figure 5 and Table 3); furthermore, the peptides belonging to each rI_{Na} size category were the same for $Na_V1.2$ and $Na_V1.4$.

The rI_{Na} with ddKIIIA, like that with native KIIIA, was smaller with $Na_V1.4$ than $Na_V1.2$. However, for the rest of the peptides, the rI_{Na} with $Na_V1.4$ was approximately the same or greater than that with $Na_V1.2$. A detailed examination of the rI_{Na} with $Na_V1.4$ was not performed, as it was for $Na_V1.2$, for mainly two reasons. First, the ddKIIIA analogues had much lower affinities for $Na_V1.4$; therefore, accurate measurements of rI_{Na} required very high concentrations ($> 100\ \mu$M) of the peptides, and such amounts were unavailable because of the cost. Moreover, the peptides' off rates with $Na_V1.4$ were larger than those with $Na_V1.2$ by 1 order of magnitude or more, and this made the assessment of the formation of peptide·TTX·$Na_V1.4$ ternary complexes problematic.

Properties of KIIIA[K7D]. We previously compared the affinities and efficacies of KIIIA and KIIIA[K7A] (*18*). In the work presented here, we also synthesized and examined KIIIA-[K7D] to document the consequences of having a negatively charged residue at position 7 in the native peptide. The kinetic constants, affinities, and efficacies of KIIIA[K7D] in blocking $Na_V1.2$ or $Na_V1.4$ are listed, along with those of KIIIA and KIIIA[K7A], in Tables 1−4.

DISCUSSION

Comparison of Disulfide-Depleted KIIIA with KIIIA. The use of ddKIIIA as a core structure for these experiments was motivated by the observation that the structures and functional activities of KIIIA and its disulfide-depleted counterpart, KIIIA-[C1A,C9A], are much the same (*20*, *27*); that is, (1) the solution structures of both peptides are quite similar, indicating that the Cys1−Cys9 disulfide bond could be removed without significant distortion of the α-helix bearing the known key residues, and (2) the rank order of potency of KIIIA[C1A,C9A] in blocking the sodium currents of all six Na_V isoforms tested was essentially the same as that of KIIIA. Thus, we concluded that the key residues for VGSC binding resided mostly on an α-helix in the C-terminal

Table 2: Rate Constants of Block of rI_{Na} by TTX and Recovery from Block following Simultaneous Washout of the TTX and Peptide

peptide	[TTX] (μM)	k_{obs} of block of rI_{Na} by TTX (min^{-1})	k_{off} of peptide·TTX·Na_V[a] (min^{-1})	k_{off} of peptide·Na_V[b] (min^{-1})	estimated k_{on}[c] (μM^{-1} min^{-1})	estimated k_{on}[d] (μM^{-1} min^{-1})
ddKIIIA	100	0.44 ± 0.13	0.58 ± 0.03	0.01 ± 0.0015	−0.0014 ± 0.0013[e]	0.0044 ± 0.0013
ddKIIIA[K7A]	10	4.4 ± 1.3	0.27 ± 0.035	0.13 ± 0.03	0.41 ± 0.13	0.44 ± 0.13
ddKIIIA[K7D]	10	1.7 ± 0.4	0.081 ± 0.013	0.083 ± 0.02	0.16 ± 0.04	0.17 ± 0.04
ddKIIIA[K7S]	10	4.6 ± 1.6	0.13 ± 0.015	0.11 ± 0.02	0.45 ± 0.16	0.46 ± 0.16
ddKIIIA[K7F]	10	2.2 ± 0.5	0.27 ± 0.01	0.3 ± 0.04	0.19 ± 0.05	0.22 ± 0.05
ddKIIIA[K7G]	3.3[f]	6.5 ± 1.0	0.48 ± 0.085	0.67 ± 0.11	1.82 ± 0.3	1.97 ± 0.3
ddKIIIA[K7L]	10	0.73 ± 0.06	0.17 ± 0.01	0.2 ± 0.009	0.056 ± 0.006	0.073 ± 0.006
ddKIIIA[K7V]	10	1.2 ± 0.05	0.082 ± 0.01	0.091 ± 0.014	0.11 ± 0.005	0.12 ± 0.005
ddKIIIA[K7T]	10	1.3 ± 0.2	0.1 ± 0.009	0.09 ± 0.006	0.12 ± 0.02	0.13 ± 0.02
ddKIIIA[K7dap]	3.3[f]	1.8 ± 0.5	0.55 ± 0.02	0.06 ± 0.008	0.38 ± 0.15	0.54 ± 0.15
KIIIA[g]	NA[h]	NA[h]	0.017 ± 0.002	0.0016 ± 0.0016	0.3 ± 0.03[i]	NA[h]
KIIIA[K7A][g]	NA[h]	NA[h]	0.024 ± 0.004	0.015 ± 0.005	0.13 ± 0.006[i]	NA[h]
KIIIA[K7D]	10	2.3 ± 0.6	0.01 ± 0.003	0.008 ± 0.001	0.23 ± 0.06	0.23 ± 0.06

[a]Rate constant of recovery from block of the peptide·TTX·Na_V1.2 ternary complex, when both peptide and TTX were simultaneously washed out. [b]Binary complex values from Table 1, reproduced here for ready comparison with ternary complex values. [c]Calculated assuming bimolecular reaction kinetics [$k_{on} = (k_{obs} - k_{off})/[TTX]$] and TTX dissociated from the peptide·TTX·Na_V ternary complex with a rate constant no larger than the k_{off} of the peptide·TTX·Na_V complex (i.e., fourth column). The rationale for this assumption is that if during the washout of both toxins TTX dissociated from the complex before the peptide did, then a rapid recovery of rI_{Na} would be expected, followed by the slower recovery from block by peptide alone; instead, the recovery from block followed essentially a single-exponential time course (see Figure 4C,D). For the most part, the k_{off} value for a given peptide·TTX·Na_V ternarycomplex was either larger or approximately equal to the k_{off} for the corresponding peptide·Na_V binary complex (compare columns 4 and 5). [d]Upper limit of k_{on} obtained by assuming TTX could not dissociate from the ternary complex, in which case estimated $k_{on} = k_{obs}/[TTX]$. Note that both estimates of k_{on} gave similar values. [e]A negative value for the estimated k_{on} suggests k_{off} of recovery from block of the ternary complex is a gross overestimate of k_{off} of TTX in this instance. [f]A lower concentration, compared to other cases, was used because of a larger relative k_{obs}. [g]Data from ref *18*. [h]Not available. [i]Obtained from the slope of the plot of k_{obs} vs ligand concentration.

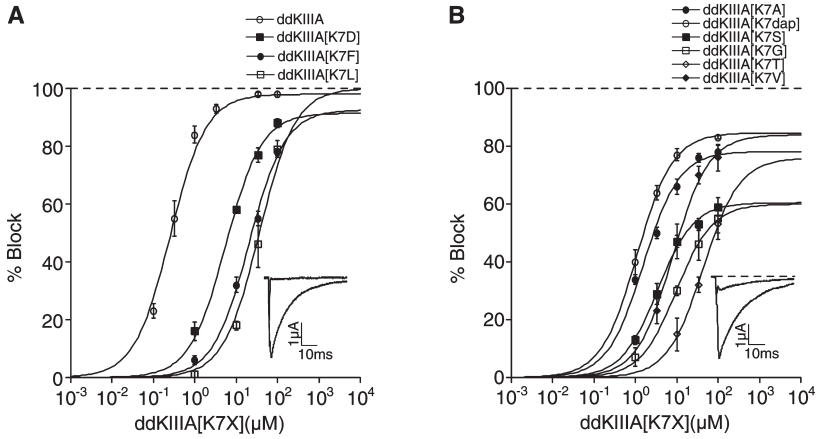

FIGURE 5: Saturating concentrations of ddKIIIA and ddKIIIA[K7X] block $Na_V1.4$ incompletely. Superimposed plots for analogues with small (< 9%) rI_{Na} values, where X is K, D, F, or L (A), and large (16−42%) rI_{Na} values, where X is A, S, G, V, T, or dap (B). Data were acquired and plotted as described in the legend of Figure 2. Except for ddKIIIA, data points of peptides do not extend to saturating concentrations because of supply limitations; thus, rI_{Na} values were obtained from plateaus extrapolated by curve fitting. Resulting IC_{50} and rI_{Na} values are listed in Table 3. The insets show representative traces in response to a depolarizing step to −10 mV from a holding potential of −80 mV before treatment (control, large trace) or in the presence of (attenuated trace) either 10 μM ddKIIIA (A) or 30 μM ddKIIIA[K7A] (B); the zero-current level is shown by the dashed line in panel B but not shown in panel A because the peptide-attenuated current trace would obscure it.

half of the peptide and that the first disulfide bond can be removed without significantly affecting the structure of this helix (*27*).

More recently, the replacement of one of the two remaining disulfide bridges of the disulfide-depleted KIIIA[C1A,C9A] with a diselenide bridge to yield the "ddKIIIA" of this work simplified the synthesis of the core structure even further (*25*). The activities of KIIIA, KIIIA[K7A], KIIIA[K7D], and their disulfide-depleted counterparts on $Na_V1.2$ are summarized in Table 4. ddKIIIA (i.e., ddKIIIA[2−5U]) and ddKIIIA[2−5C] had similar K_d values (13 and 7.8 nM, respectively), with the former having slower k_{on} and k_{off} values than the latter. Since the substitution of the disulfide bridge with a diselenide bridge had an only minimal effect, we felt justified in using the peptide with the diselenide bridge as the core structure for positional scanning studies, particularly in view of the vastly accelerated synthesis of its analogues. This view is further supported by the observation that the functional differences between ddKIIIA[K7A] and ddKIIIA found in this study paralleled those between KIIIA[K7A] and KIIIA (*18*).

To further investigate the role of electrical charge at position 7 of KIIIA, KIIIA[K7D] was tested for comparison with KIIIA and KIIIA[K7A], as well as with ddKIIIA[K7A]. In each case, whether KIIIA[K7X] or ddKIIIA[K7X], the major effect of replacing Lys7 with Ala or Asp was an ~10-fold increase in k_{off} (Table 1). The rI_{Na} levels with KIIIA, KIIIA[K7A], and KIIIA-[K7D] mirrored those of their respective disulfide-deficient counterparts, as discussed further below. Finally, TTX blocked

Table 3: Kinetics, Affinities, and Efficacies of ddKIIIA Analogues in Blocking $Na_V1.4$[a]

peptide	k_{on} (μM^{-1} min^{-1})	k_{off} (min^{-1})	IC_{50} (μM) (95% confidence interval)	rI_{Na} (%)[b]
ddKIIIA	1.4 ± 0.15	0.36 ± 0.06	0.25 (0.22−0.29)	2 ± 1.0
ddKIIIA[K7A]	0.17 ± 0.03	1.2 ± 0.3	1.6 (1.3−1.9)	22 ± 2.3
ddKIIIA[K7D]	0.18 ± 0.02	1.5 ± 0.3	5.6 (4.7−6.6)	9 ± 2.6
ddKIIIA[K7S]	NA[c]	2.4 ± 0.7	3.4 (2.8−4.1)	40 ± 2.3
ddKIIIA[K7F]	NA[c]	4.6 ± 1.0	20 (17−25)	7 ± 4.7
ddKIIIA[K7G]	NA[c]	6.9 ± 1.6	9.8 (6.0−16)	40 ± 6.0
ddKIIIA[K7L]	NA[c]	9.5 ± 3.8	36 (30−44)	–[d]
ddKIIIA[K7V]	NA[c]	2.6 ± 0.8	8.1 (6.0−11)	16 ± 5.2
ddKIIIA[K7T]	NA[c]	2.8 ± 0.7	45.3 (26−78)	23 ± 13
ddKIIIA[K7dap]	NA[c]	3.1 ± 0.8	1.1 (0.92−1.3)	16 ± 2.2
KIIIA	0.97 ± 0.09	0.047 ± 0.015	0.082 (0.067−0.1)	1 ± 0.6
KIIIA[K7A]	0.36 ± 0.08	0.37 ± 0.08	1.1 (0.95−1.3)	30 ± 2.1
KIIIA[K7D]	0.11 ± 0.015	0.15 ± 0.02	1.5 (1.1−2.0)	6 ± 3.5

[a]Kinetic and steady-state values were obtained as described in Table 1, and data are partially illustrated in Figure 5. For comparison, also shown are data for KIIIA, KIIIA[K7D], and KIIIA[K7A] from experiments performed for this report. [b]Values of rI_{Na} were directly obtained at saturating peptide concentrations for ddKIIIA, KIIIA, and KIIIA[K7A], and for the remaining peptides, curve-fit plateau values were used to provide estimates of rI_{Na}, because low affinities experienced with $Na_V1.4$ required concentrations of peptide of > 100 μM to fully saturate $Na_V1.4$. Such concentrations called for quantities of peptides unavailable to us. [c]The on rate was too fast to be accurately measured at the high peptide concentrations necessary to observe significant block of sodium current. [d]The curve-fit plateau value was $> 100\%$; therefore, no estimate of rI_{Na} is given.

Table 4: Comparison of kinetics of TTX- or peptide-block of $Na_V1.2$ and of TTX-block of binary peptide•$Na_V1.2$ complexes

ligand	target	k_{on} (μM^{-1} min^{-1})	k_{off} (min^{-1})	K_d (nM)	ref
TTX	$Na_V1.2$	58 ± 5.3[b]	2.2 ± 0.3	38 ± 6	*18*
KIIIA	$Na_V1.2$	0.3 ± 0.03[b]	0.0016 ± 0.0016	5.3 ± 5	*18*
KIIIA[K7A]	$Na_V1.2$	0.13 ± 0.006[b]	0.015 ± 0.005	115 ± 38	*18*
KIIIA[K7D]	$Na_V1.2$	0.02 ± 0.002	0.008 ± 0.001	0.4 ± 0.06	this report
ddKIIIA[2−5C][a]	$Na_V1.2$	1.8 ± 0.39[c]	0.014 ± 0.002	7.8 ± 2	*27*
ddKIIIA	$Na_V1.2$	0.75 ± 0.015[b]	0.01 ± 0.0015	13 ± 2	this report
ddKIIIA[K7A]	$Na_V1.2$	0.69 ± 0.11[b]	0.13 ± 0.03	190 ± 50	this report
ddKIIIA[K7D]	$Na_V1.2$	0.08 ± 0.005	0.083 ± 0.02	1.04 ± 0.26	this report
TTX	KIIIA·$Na_V1.2$	0.003 ± 0.0004[b]	NA[d]	NA[d]	*18*
TTX	KIIIA[K7A]·$Na_V1.2$	0.56 ± 0.08[b]	NA[d]	NA[d]	*18*
TTX	KIIIA[K7D]·$Na_V1.2$	0.23 ± 0.06[c]	NA[d]	NA[d]	this report
TTX	ddKIIIA·$Na_V1.2$	0.0044 ± 0.0013[c]	NA[d]	NA[d]	this report
TTX	ddKIIIA[K7A]·$Na_V1.2$	0.44 ± 0.13[c]	NA[d]	NA[d]	this report
TTX	ddKIIIA[K7D]·$Na_V1.2$	0.17 ± 0.04[c]	NA[d]	NA[d]	this report

[a]ddKIIIA[2−5C] is ddKIIIA with a disulfide, instead of diselenide, bridge (i.e., KIIIA[C1A,C9A]). [b]Obtained from the slope of the plot of k_{obs} vs ligand concentration. [c]Obtained from k_{obs} at a single ligand concentration (see Table 2). [d]Value not available, because it could not be directly determined experimentally.

the rI_{Na} of $Na_V1.2$ with either KIIIA or ddKIIIA at approximately the same rate, which was ~300-fold slower than that with either KIIIA[K7D] or ddKIIIA[K7D] and ~100-fold slower than that with either KIIIA[K7A] or ddKIIIA[K7A]; these in turn were 100−300-fold slower than the rate at which TTX blocked the control I_{Na} (compare the k_{on} data in the first row and last six rows of Table 4). In summary, for each pair tested on $Na_V1.2$, when ddKIIIA[K7X] is compared to its KIIIA[K7X] counterpart, when X is K, A, and D, (1) k_{on} is larger by factors ranging from 2.5 to 5.3, (2) k_{off} is larger by a factor ranging from 6.2 to 10, (3) K_d is larger by a factor ranging from 1.6 to 2.6, (4) efficacy (or rI_{Na}) changes by ≤17%, and (5) the rate of TTX block of rI_{Na} differs by only 1.3−1.5-fold. Thus, the alteration of functional parameters upon conversion of "native peptide" to "dd peptide" occurred in a parallel fashion for all three pairs of peptides.

Kinetics and Affinities in the Formation of ddKIIIA-[K7X]·$Na_V1.2$ Binary Complexes. Positional scanning of Lys7 of ddKIIIA with the nine amino acids tested revealed that affinity could be attenuated to varying degrees (Figures 2 and 5). In all cases, k_{off} was increased (Tables 1 and 3), consistent with the notion that the loss of the positive charge of Lys destabilized the bound complex (*18*); dap also has a positive charge, but on a much shorter side chain than Lys, and the dap-containing analogue had the lowest k_{off} after ddKIIIA when tested against $Na_V1.2$ (but not $Na_V1.4$). Note, however, the analogue with reversed charge, ddKIIIA[K7D], did not have the fastest k_{off} of the peptides tested against $Na_V1.2$, although it had the slowest k_{on} (Table 1).

Compared to KIIIA, KIIIA[K7A], and KIIIA[K7D], most ddKIIIA analogues had a larger k_{on}. A possible explanation for this is that the disulfide deficiency endowed the peptides with greater structural flexibility, and therefore, they more readily assumed a conformation that favored a faster on rate, as we previously speculated (*27*).

Like KIIIA, ddKIIIA blocked with an rI_{Na} that was small: 5% on $Na_V1.2$ (Table 1) and ~2% on $Na_V1.4$ (Table 3). KIIIA[K7D] had a small rI_{Na} of 6% on $Na_V1.2$ and 1.4 (Tables 1 and 4, respectively), and ddKIIIA[K7D] also blocked $Na_V1.2$ and $Na_V1.4$ with a small rI_{Na} [5 and 9%, respectively (Tables 1 and 4)]. In contrast, the K7A analogues of each of these produced

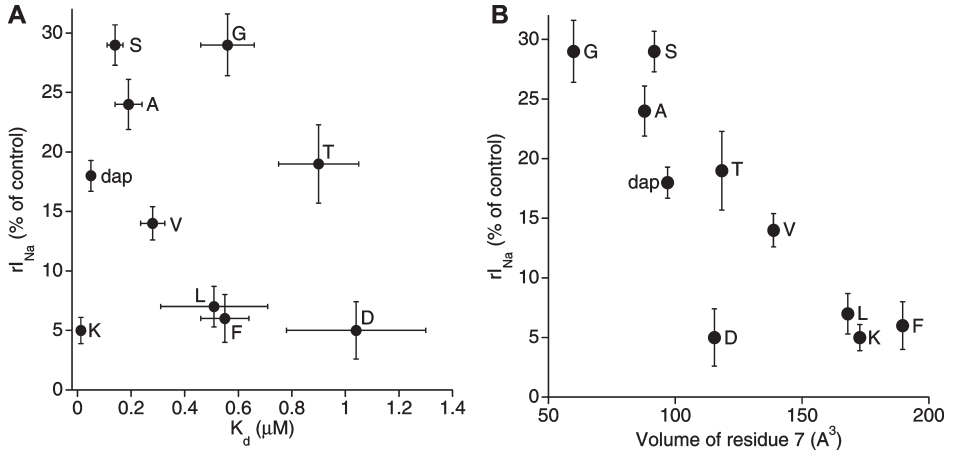

FIGURE 6: Relationships between $Na_V1.2$ rI_{Na} vs K_d and volume of residue 7 of ddKIIIA[K7X]. Plots of data in Table 1. Each data point is labeled with the amino acid corresponding to residue 7 of ddKIIIA[K7X]. (A) A plot of rI_{Na} vs K_d shows that efficacy and affinity are apparently uncorrelated. (B) A plot of rI_{Na} vs volume of residue 7 shows that rI_{Na} varies inversely with size of the residue; remarkably, rI_{Na} seems to be insensitive to side chain charge or hydrophobicity. AA volumes are from Table 1 of ref *38*; dap volume was estimated by subtracting the volume of three methylene groups from the volume of Lys, where the volume of a methylene group was estimated from the average difference in volume between Glu and Asp and between Gln and Asn.

an rI_{Na} that was large: 23% with KIIIA[K7A] and 24% with ddKIIIA[K7A] on $Na_V1.2$ (Table 1) and 30% with KIIIA-[K7A] and 22% with ddKIIIA[K7A] on $Na_V1.4$ (Table 3). Thus, the disulfide deficiency affected the efficacies of these peptides only marginally.

Residual Currents Correlate Inversely with the Size of the Residue at Position 7. The rI_{Na} values of ddKIIIA[K7X] did not seem to correlate with either their affinities (Figure 6A), their k_{on} values, or their k_{off} values (Tables 1 and 3); instead, rI_{Na} correlated inversely with the size of the side chain of residue 7, with both $Na_V1.2$ (Figure 6B) and $Na_V1.4$ (not graphically illustrated, but see Table 3). Thus, the impediment to passage of sodium ions increased as the size of residue 7 of the bound peptide increased.

The correlation of blocking efficacy with side chain size is reminiscent of the actions of μ-conotoxin GIIIA[R13X] mutants on $Na_V1.4$, where X was one of seven residues with different side chain lengths and charges; for a given charge, efficacy progressively increased with length, and for a given length, efficacy progressively increased as the charge was varied from -1, 0, to 1 (*28*). This last behavior differs from that of the ddKIIIA[K7X] analogues, for which charge was largely immaterial, and suggests that functionally Lys7 of KIIIA is not strictly homologous to Arg13 of GIIIA.

Block of rI_{Na} by TTX. In all cases, the presence of the bound peptide increased not only the impediment to passage of Na^+ but apparently also that of TTX. That is, TTX blocked the rI_{Na} with ddKIIIA and all ddKIIIA[K7X] derivatives at a rate significantly slower than the control I_{Na} (Figure 4 and Table 2). Thus, TTX appears to be able to "sneak by" the bound peptides only with difficulty and block the residual current, which was originally suggested to occur with KIIIA and KIIIA[K7A] (*18*).

When the rates of TTX block of the rI_{Na} are compared with the magnitudes of the rI_{Na} values, a positive correlation is evident (Figure 7). Among the peptides with a small rI_{Na} ($\leq$7% of control), TTX's k_{on} appears to depend on charge, suggesting that an electrostatic attraction between the positively charged guanidinium of TTX and the negativity of Asp and the π-electrons of Phe may account for the elevated values of k_{on} for the mutants with those residues. In this regard, it might be noted that a

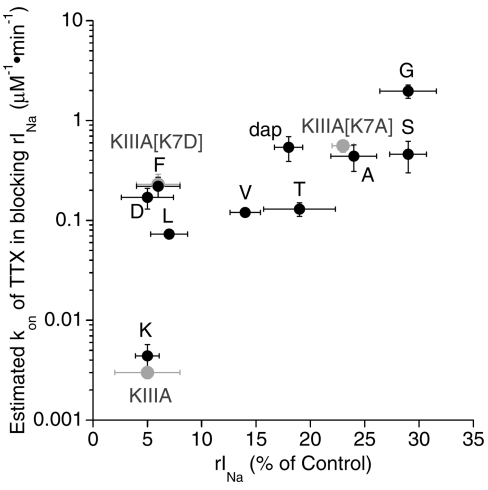

FIGURE 7: Relationship between the susceptibility of rI_{Na} to be blocked by TTX and the size of residue 7 of ddKIIIA[K7X]. The value of k_{on} for block of rI_{Na} with $Na_V1.2$ by TTX was estimated from the observed rate constant of block (k_{obs}) of rI_{Na} at a single concentration of TTX and assuming k_{off} to be zero (see the last column of Table 2). Data points are labeled as in Figure 6. The plot suggests a general tendency that the smaller the rI_{Na}, the more TTX is impeded. Gray circles represent data for KIIIA and KIIIA[K7A] from ref *18*, and KIIIA[K7D] (Tables 1 and 4); note that the data point for each peptide lies close to that of its disulfide-depleted counterpart.

cation$-\pi$-electron interaction is observed between Tyr401 of $Na_V1.4$ and bound TTX (*29*); furthermore, the $Na_V1.4$[Y401C] mutation results in a very large decrease in TTX affinity that is mostly due to a decrease in the k_{on} of TTX (*30*). Conversely, the very low k_{on} value of TTX with bound KIIIA or ddKIIIA may be a reflection of the positive charge of Lys7, which would repel TTX. Note, however, dap, although positively charged, did not retard TTX strongly, possibly because the ammonium group of dap is on a very short tether compared to that of Lys; i.e., one versus four methylene groups link the α-carbon with the side chain ammonium group.

Stability of the Peptide·TTX·$Na_V1.2$ Ternary Complex. The presence of TTX accelerated the unbinding of KIIIA from $Na_V1.2$ by a factor of 10 (*18*), and such an effect of TTX was

also only evident with ddKIIIA and ddKIIIA[K7X] when X was dap (compare columns 4 and 5 of Table 2). The destabilizing effect of TTX is consistent with an electrostatic repulsion between the positive charge of TTX and that at residue 7 in the peptide. The minimal effect the charge on dap had in retarding TTX block, as discussed above, suggests that the impediment to passage of TTX is sensitive to the position of the positive charge at residue 7, whereas the destabilization of the ternary complex is relatively insensitive to the position of the charge. It might be noted that the k_{off} of ddKIIIA[K7D] (where Asp confers a negative charge at residue 7) was the same whether TTX was present, but this could be a reflection of the relatively slow k_{off} of ddKIIIA[K7D] from $Na_V1.2$ to begin with (Table 2).

In the experiments thus far, only position 7 of KIIIA was scrutinized, and further experiments are necessary to obtain a clearer picture of the structural elements of the peptide responsible for its affinity for the channel and its efficacy in interfering with TTX block versus sodium permeation. Positional scanning at other locations with positively charged residues, such as R10 and R14, may be enlightening in this regard. Furthermore, determination of the Na_V subtype selectivity profiles of the various derivatives of KIIIA would be informative, particularly since the channel(s) responsible for KIIIA's analgesic activity (*17*) remains unidentified.

Exploiting μ-Conopeptides That Have Limited Efficacies. The possibility of independently manipulating the affinity and efficacy of a pore-blocking ligand of VGSCs is of interest for the development of possible drugs for therapeutic intervention. Consider a μ-conopeptide that has been engineered to have (1) high affinity for VGSCs, (2) highly attenuated efficacy in blocking I_{Na}, and (3) high efficacy in retarding the block by TTX. Such a peptide could serve as a contratoxin, or antidote, against tetrodotoxin poisoning (*18*). The analogues with the lowest efficacy against $Na_V1.4$ were ddKIIIA[K7G] and ddKIIIA[K7S], with rI_{Na} values near 40% (Table 3). It would be interesting to see if these are able to shield the channel against TTX and therefore prevent TTX from blocking action potentials in adult skeletal muscle, which normally have $Na_V1.4$ exclusively (*31*), a situation that might be expected in muscle fibers with a safety factor of greater than 2 for action potential propagation.

The possibility of using TTX and STX congeners as local analgesic agents has recently been explored (*32*−*34*). However, for more general therapeutic use of VGSC blockers, a major quandary is that all but two of the mammalian Na_V1 isoforms appear to be critical for survival. The exceptions are $Na_V1.8$ and $Na_V1.9$, which apparently serve largely in the signaling of nociceptive information and for which null mouse mutations are nonlethal (*35*, *36*). Thus, to be therapeutically useful, a VGSC blocker should not have only appropriate subtype selectivity, but its dosage must also be carefully regulated. The latter constraint may be circumvented by development of a selective μ-conopeptide that has been engineered to have high affinity but reduced efficacy. Such a drug would be expected to have a large therapeutic index and may be of use to treat the signs of gain-of-function channelopathies such as those implicated in some epilepsies and pain disorders (*37*).

ACKNOWLEDGMENT

We thank Prof. Alan Goldin for providing the Na_V clones and Dr. Layla Azam for producing cRNA from them. We also thank Drs. Robert Schackmann and Scott Endicott from the DNA/Peptide Synthesis Core Facility at the University of Utah for the synthesis of peptides in general and Corey Jensen for the synthesis of ddKIIIA[K7D]. B.M.O. is a cofounder of Cognetix, Inc. G.B. is a cofounder of NeuroAdjuvants, Inc.

REFERENCES

1. Hille, B. (2001) Ion Channels of Excitable Membranes, 3rd ed., Sinauer Associates, Sunderland, MA.
2. Catterall, W. A., Goldin, A. L., and Waxman, S. G. (2005) International Union of Pharmacology. XLVII. Nomenclature and structure-function relationships of voltage-gated sodium channels. *Pharmacol. Rev. 57*, 397–409.
3. Brackenbury, W. J., and Isom, L. L. (2008) Voltage-gated Na^+ channels: Potential for β subunits as therapeutic targets. *Expert Opin. Ther. Targets 12*, 1191–1203.
4. Yu, F. H., and Catterall, W. A. (2003) Overview of the voltage-gated sodium channel family. *Genome Biol. 4*, 207.
5. Billen, B., Bosmans, F., and Tytgat, J. (2008) Animal peptides targeting voltage-activated sodium channels. *Curr. Pharm. Des. 14*, 2492–2502.
6. Daly, J. W. (2004) Marine toxins and nonmarine toxins: Cconvergence or symbiotic organisms? *J. Nat. Prod. 67*, 1211–1215.
7. Fry, B. G., Roelants, K., Champagne, D. E., Scheib, H., Tyndall, J. D., King, G. F., Nevalainen, T. J., Norman, J. A., Lewis, R. J., Norton, R. S., Renjifo, C., and de la Vega, R. C. (2009) The toxicogenomic multiverse: Convergent recruitment of proteins into animal venoms. *Annu. Rev. Genomics Hum. Genet. 10*, 483–511.
8. Terlau, H., and Olivera, B. M. (2004) *Conus* venoms: A rich source of novel ion channel-targeted peptides. *Physiol. Rev. 84*, 41–68.
9. French, R. J., and Terlau, H. (2004) Sodium channel toxins: Receptor targeting and therapeutic potential. *Curr. Med. Chem. 11*, 3053–3064.
10. Wood, J. N., Boorman, J. P., Okuse, K., and Baker, M. D. (2004) Voltage-gated sodium channels and pain pathways. *J. Neurobiol. 61*, 55–71.
11. Fiedler, B., Zhang, M. M., Buczek, O., Azam, L., Bulaj, G., Norton, R. S., Olivera, B. M., and Yoshikami, D. (2008) Specificity, affinity and efficacy of ι-conotoxin RXIA, an agonist of voltage-gated sodium channels Na(V)1.2, 1.6 and 1.7. *Biochem. Pharmacol. 75*, 2334–2344.
12. Cestele, S., and Catterall, W. A. (2000) Molecular mechanisms of neurotoxin action on voltage-gated sodium channels. *Biochimie 82*, 883–892.
13. Cruz, L. J., Gray, W. R., Olivera, B. M., Zeikus, R. D., Kerr, L., Yoshikami, D., and Moczydlowski, E. (1985) *Conus geographus* toxins that discriminate between neuronal and muscle sodium channels. *J. Biol. Chem. 260*, 9280–9288.
14. Moczydlowski, E., Olivera, B. M., Gray, W. R., and Strichartz, G. R. (1986) Discrimination of muscle and neuronal Na-channel subtypes by binding competition between [^{3}H]saxitoxin and μ-conotoxins. *Proc. Natl. Acad. Sci. U.S.A. 83*, 5321–5325.
15. Sato, K., Ishida, Y., Wakamatsu, K., Kato, R., Honda, H., Ohizumi, Y., Nakamura, H., Ohya, M., Lancelin, J. M., and Kohda, D.; et al. (1991) Active site of μ-conotoxin GIIIA, a peptide blocker of muscle sodium channels. *J. Biol. Chem. 266*, 16989–16991.
16. Bulaj, G., West, P. J., Garrett, J. E., Watkins, M., Zhang, M. M., Norton, R. S., Smith, B. J., Yoshikami, D., and Olivera, B. M. (2005) Novel conotoxins from *Conus striatus* and *Conus kinoshitai* selectively block TTX-resistant sodium channels. *Biochemistry 44*, 7259–7265.
17. Zhang, M. M., Green, B. R., Catlin, P., Fiedler, B., Azam, L., Chadwick, A., Terlau, H., McArthur, J. R., French, R. J., Gulyas, J., Rivier, J. E., Smith, B. J., Norton, R. S., Olivera, B. M., Yoshikami, D., and Bulaj, G. (2007) Structure/function characterization of μ-conotoxin KIIIA, an analgesic, nearly irreversible blocker of mammalian neuronal sodium channels. *J. Biol. Chem. 282*, 30699–30706.
18. Zhang, M. M., McArthur, J. R., Azam, L., Bulaj, G., Olivera, B. M., French, R. J., and Yoshikami, D. (2009) Synergistic and antagonistic interactions between tetrodotoxin and μ-conotoxin in blocking voltage-gated sodium channels. *Channels* (*Austin, TX*) *3*, 32–38.
19. French, R. J., Prusak-Sochaczewski, E., Zamponi, G. W., Becker, S., Kularatna, A. S., and Horn, R. (1996) Interactions between a pore-blocking peptide and the voltage sensor of the sodium channel: An electrostatic approach to channel geometry. *Neuron 16*, 407–413.
20. Han, T. S., Zhang, M. M., Walewska, A., Gruszczynski, P., Robertson, C. R., Cheatham, T. E., III, Yoshikami, D., Olivera, B. M., and Bulaj, G. (2009) Structurally minimized μ-conotoxin analogues as sodium channel blockers: Implications for designing conopeptide-based therapeutics. *ChemMedChem 4*, 406–414.

21. Walewska, A., Zhang, M. M., Skalicky, J. J., Yoshikami, D., Olivera, B. M., and Bulaj, G. (2009) Integrated oxidative folding of cysteine/selenocysteine containing peptides: Improving chemical synthesis of conotoxins. *Angew. Chem., Int. Ed. 48*, 2221–2224.
22. Armishaw, C. J., Daly, N. L., Nevin, S. T., Adams, D. J., Craik, D. J., and Alewood, P. F. (2006) α-Selenoconotoxins, a new class of potent α7 neuronal nicotinic receptor antagonists. *J. Biol. Chem. 281*, 14136–14143.
23. Gowd, K. H., Yarotskyy, V., Elmslie, K. S., Skalicky, J. J., Olivera, B. M., and Bulaj, G. (2010) Site-specific effects of diselenide bridges on the oxidative folding of a cystine knot peptide, ω-selenoconotoxin GVIA. *Biochemistry 49*, 2741–2752.
24. Muttenthaler, M., Nevin, S. T., Grishin, A. A., Ngo, S. T., Choy, P. T., Daly, N. L., Hu, S. H., Armishaw, C. J., Wang, C. I., Lewis, R. J., Martin, J. L., Noakes, P. G., Craik, D. J., Adams, D. J., and Alewood, P. F. (2010) Solving the α-conotoxin folding problem: Efficient selenium-directed on-resin generation of more potent and stable nicotinic acetylcholine receptor antagonists. *J. Am. Chem. Soc. 132*, 3514–3522.
25. Han, T. S., Zhang, M. M., Gowd, K. H., Walewska, A., Yoshikami, D., Olivera, B. M., and Bulaj, G. (2010) Disulfide-Depleted Selenoconopeptides: Simplified Oxidative Folding of Cysteine-Rich Peptides. *ACS Med. Chem. Lett. 1*, DOI: 10.1021/ml900017q.
26. West, P. J., Bulaj, G., Garrett, J. E., Olivera, B. M., and Yoshikami, D. (2002) μ-Conotoxin SmIIIA, a potent inhibitor of tetrodotoxin-resistant sodium channels in amphibian sympathetic and sensory neurons. *Biochemistry 41*, 15388–15393.
27. Khoo, K. K., Feng, Z. P., Smith, B. J., Zhang, M. M., Yoshikami, D., Olivera, B. M., Bulaj, G., and Norton, R. S. (2009) Structure of the analgesic μ-conotoxin KIIIA and effects on the structure and function of disulfide deletion. *Biochemistry 48*, 1210–1219.
28. Hui, K., Lipkind, G., Fozzard, H. A., and French, R. J. (2002) Electrostatic and steric contributions to block of the skeletal muscle sodium channel by μ-conotoxin. *J. Gen. Physiol. 119*, 45–54.
29. Santarelli, V. P., Eastwood, A. L., Dougherty, D. A., Horn, R., and Ahern, C. A. (2007) A cation-π interaction discriminates among sodium channels that are either sensitive or resistant to tetrodotoxin block. *J. Biol. Chem. 282*, 8044–8051.
30. Penzotti, J. L., Fozzard, H. A., Lipkind, G. M., and Dudley, S. C., Jr. (1998) Differences in saxitoxin and tetrodotoxin binding revealed by mutagenesis of the Na^+ channel outer vestibule. *Biophys. J. 75*, 2647–2657.
31. Trimmer, J. S., Cooperman, S. S., Agnew, W. S., and Mandel, G. (1990) Regulation of muscle sodium channel transcripts during development and in response to denervation. *Dev. Biol. 142*, 360–367.
32. Lattes, K., Venegas, P., Lagos, N., Lagos, M., Pedraza, L., Rodriguez-Navarro, A. J., and Garcia, C. (2009) Local infiltration of gonyautoxin is safe and effective in treatment of chronic tension-type headache. *Neurol. Res. 31*, 228–233.
33. Marcil, J., Walczak, J. S., Guindon, J., Ngoc, A. H., Lu, S., and Beaulieu, P. (2006) Antinociceptive effects of tetrodotoxin (TTX) in rodents. *Br. J. Anaesth. 96*, 761–768.
34. Rodriguez-Navarro, A. J., Lagos, N., Lagos, M., Braghetto, I., Csendes, A., Hamilton, J., Figueroa, C., Truan, D., Garcia, C., Rojas, A., Iglesias, V., Brunet, L., and Alvarez, F. (2007) Neosaxitoxin as a local anesthetic: Preliminary observations from a first human trial. *Anesthesiology 106*, 339–345.
35. Akopian, A. N., Souslova, V., England, S., Okuse, K., Ogata, N., Ure, J., Smith, A., Kerr, B. J., McMahon, S. B., Boyce, S., Hill, R., Stanfa, L. C., Dickenson, A. H., and Wood, J. N. (1999) The tetrodotoxin-resistant sodium channel SNS has a specialized function in pain pathways. *Nat. Neurosci. 2*, 541–548.
36. Amaya, F., Wang, H., Costigan, M., Allchorne, A. J., Hatcher, J. P., Egerton, J., Stean, T., Morisset, V., Grose, D., Gunthorpe, M. J., Chessell, I. P., Tate, S., Green, P. J., and Woolf, C. J. (2006) The voltage-gated sodium channel $Na_v1.9$ is an effector of peripheral inflammatory pain hypersensitivity. *J. Neurosci. 26*, 12852–12860.
37. Catterall, W. A., Dib-Hajj, S., Meisler, M. H., and Pietrobon, D. (2008) Inherited neuronal ion channelopathies: New windows on complex neurological diseases. *J. Neurosci. 28*, 11768–11777.
38. Perkins, S. J. (1986) Protein volumes and hydration effects. The calculations of partial specific volumes, neutron scattering match-points and 280-nm absorption coefficients for proteins and glycoproteins from amino acid sequences. *Eur. J. Biochem. 157*, 169–180.